

*Full Length Research Paper*

# Energy-efficient channel estimation for multiband UWB systems in presence of interferences

S. M. Riazul Islam\* and Kyung Sup Kwak

Telecommunication Engineering Lab, Inha University, Incheon, 402-751, South Korea.

Accepted 15 November, 2010

Interference reduces the performance of a correct data signal detection and decoding. This problem becomes severe when interferences exist during the period of channel estimation. This will destroy the accuracy of channel estimation, and will eventually result to severe degradation in the performance of signal detection and decoding in the entire data packet/frame. In this article, we propose an improved channel estimation technique for multiband orthogonal frequency division multiplexing (MB-OFDM) ultra-wideband (UWB) system in presence of interferences. In particular, we work towards a preamble-based channel estimation technique in multi-access and narrowband interfering environments. We construct two preamble symbols with opposite, both in amplitude and phase, sequences in frequency-domain. Time-domain redundancy is introduced into these preamble symbols before transmission. Based on this time-domain redundancy property, we eliminate multi-access interference (MAI) through an adaptive select and replace (ASR) scheme. We show that the use of opposite sequences in preambles leads a simple addition, subtraction and compare (ASC) scheme to cancel narrowband interference (NBI). In addition, we apply a frequency-domain filter, driven by channel's power delay profile (PDP), to get a further enhancement in the estimation accuracy. Simulation results urge that our proposed technique outperforms the conventional channel estimation methods.

**Key words:** Ultra-wideband, channel estimation, channel impulse response (CIR), multiband orthogonal frequency division multiplexing, wireless personal area network (WPAN), narrowband interference, multi-access interference, and ECMA-368.

## INTRODUCTION

The popularity of multiband orthogonal frequency division multiplexing (MB-OFDM), Ultra-wideband (UWB) system continues to grow as the physical (PHY) layer of wireless personal area network (WPAN), especially for high data rate applications in home networks. MB-OFDM has already been taken in the standard ECMA-368 (ECMA International, 2008) for high rate UWB. To operate the PHY service interface to the MAC service, ECMA-368 defines a packet layer convergence protocol (PLCP) sublayer. PLCP sublayer provides a method for converting a PLCP service data unit (PSDU) into a PLCP packet data unit (PPDU), resulting in the PPDU being composed of three components. They are the PLCP

preamble, PLCP header, and the PSDU. The PLCP preamble is the first component of the PPDU and can be further decomposed into packet/frame synchronization (PFS), and channel estimation sequences. The goal of the PLCP preamble is to aid the receiver in timing synchronization, carrier-offset recovery, and channel estimation. The PFS is either 12 (burst mode) or 24 (standard mode) zero autocorrelation stored time-domain bursts with the same timing as OFDM frames. The channel estimation sequence is actually defined in the frequency-domain and an inverse fast Fourier transform (IFFT) can be used to convert to the required time-domain for transmission. Two OFDM symbols are used as a channel estimation sequence for each band. Thus, six OFDM symbols are needed for channel estimation as the MB-OFDM system employs hopping over a maximum of 3 bands.

\*Corresponding author. Email: [riazuldu@yahoo.com](mailto:riazuldu@yahoo.com).

In MB-OFDM UWB system, piconet consists of a piconet coordinator and multiple data devices. It is assumed that there are multiple simultaneously operating piconets (SOPs) present in the same environment. Let us also assume that there is an asynchronous SOP using the band group the same as the desired piconet. In such a scenario, each preamble symbol may be partially overlapped by an interfering symbol and the resultant interference is termed multi-access interference (MAI). In the study of UWB system, narrowband implies bandwidth under consideration is "sufficiently" narrow compared to the UWB bandwidth. A wideband system, by its nature, interferes with the existing narrowband services in the same frequency band and in turn, the narrowband signals act as interferers to wideband system. This interference is termed narrowband interference (NBI). Interferences, both MAI and NBI, reduce the performance of a correct data signal detection and decoding. This problem becomes severe when interferences exist during channel estimation period. This will destroy the accuracy of channel estimation and, will eventually result severe degradation in the performance of signal detection and decoding in the entire data packet/frame.

To date, there exist several channel estimation techniques for MB-OFDM systems. However, a few of them are preamble-based approaches. Li et al. (2008) develops carrier frequency offset (CFO)-assisted CIR estimator with imperfect timing offset. The technique (Fan et al., 2005) applies rectangular windowing, with an adaptive length, on discrete fourier transform (DFT) estimator to get improved estimation performance. The work Png et al. (2008) introduces adaptive filter in the frequency-domain to reduce the mean square error (MSE) of the estimated channel. The article (Shin et al., 2007) proposes low rank linear minimum mean square error (LMMSE) channel estimation with variable rank. However, these works (Li et al., 2008; Fan et al., 2005; Png et al., 2008; Shin et al., 2007) assume interference-free environments; preambles are not hindered by interference. The work (Li et al., 2006) develops practical approaches for channel estimation and interference suppression. Yet the interference suppression method is based on interference averaging. Tasi et al. (2008) propose an adaptive channel estimation method in presence of MAI; they apply time-domain redundancy property. Yet they do not study the feasibility of estimation accuracy in presence of NBI. We find a joint NBI detection and channel estimation (Hadaschik et al., 2007); this is an iterative approach that finds the subcarrier with maximum power to consider the center frequency of the NBI. Conversely, the approach is unable to detect all affected subcarriers. Moreover, this method does not consider the existence of MAI. To the best of our knowledge, we do not find any work that investigates the estimation performance in presence of both MAI and NBI. Therefore, an improved channel estimation

technique for MB-OFDM UWB system is required with three characteristics. First, the method should be based on preambles. Second, this technique should continue to work well in presence of the MAI. Lastly, the technique should cancel the NBI from the preambles. In this article, we propose a preamble-based channel estimation technique for MB-OFDM UWB system in the presence of both MAI and NBI.

**SYSTEM MODEL**

The MB-OFDM system model of interest is depicted in Figure 1. In this model, we do not consider scrambling, puncturing and interleaving for simplicity. The information bits, with average power equal to  $E_c$ , are fed into a convolution encoder with rate, R, to provide redundancy against bad channel effects. The output of encoder is then mapped onto each subcarrier based on quadrature phase shift keying (QPSK) constellation with average power equal to  $E_s$ . The output of the constellation mapper is then passed through serial-to-parallel (S/P) converter and pilot and guard subcarriers insertion block. The frequency-domain data symbols located on the subcarriers are denoted by  $\bar{D}$  and given by,

$$\bar{D} = [D[k]]^T = [D_0, D_1, \dots, D_{N-1}]^T, \tag{1}$$

where  $(.)^T$  denotes the transpose operator and  $N$  be the number of subcarriers constituting the OFDM symbol. Note that the average power of the coded data on each tone is given by  $E_c = RE_s$ . The data symbols are subsequently modulated into time-domain samples using inverse fast Fourier transform (IFFT),

$$\bar{d} = [d[n]]^T = \left[ \frac{1}{N} \sum_{k=0}^{N-1} D[k] \cdot e^{-j2\pi n k / N} \right]^T, \quad n = 0, 1, \dots, N - 1, \tag{2}$$

A ZPS of  $Z$  samples is appended at the end of  $\bar{d}$  to give,

$$\bar{d}_{ZPS} = [d_0, d_1, \dots, d_{N-1}, d_N, d_{N+1}, \dots, d_{N+Z-1}]^T, \tag{3}$$

The ZPS is used to mitigate the effects of intersymbol interference (ISI) and intercarrier interference (ICI) caused by the channel. The digital time-domain signal given in Equation 3 is then converted to analog signal, using digital-to-analog converter (DAC), for transmission. The output of DAC is multiplied by one of the RF frequency bands scheduled by time-frequency code (TFC). However, we will present the analysis for the baseband digital part only, since we avoid RF signal processing for simplicity. The channel that we are

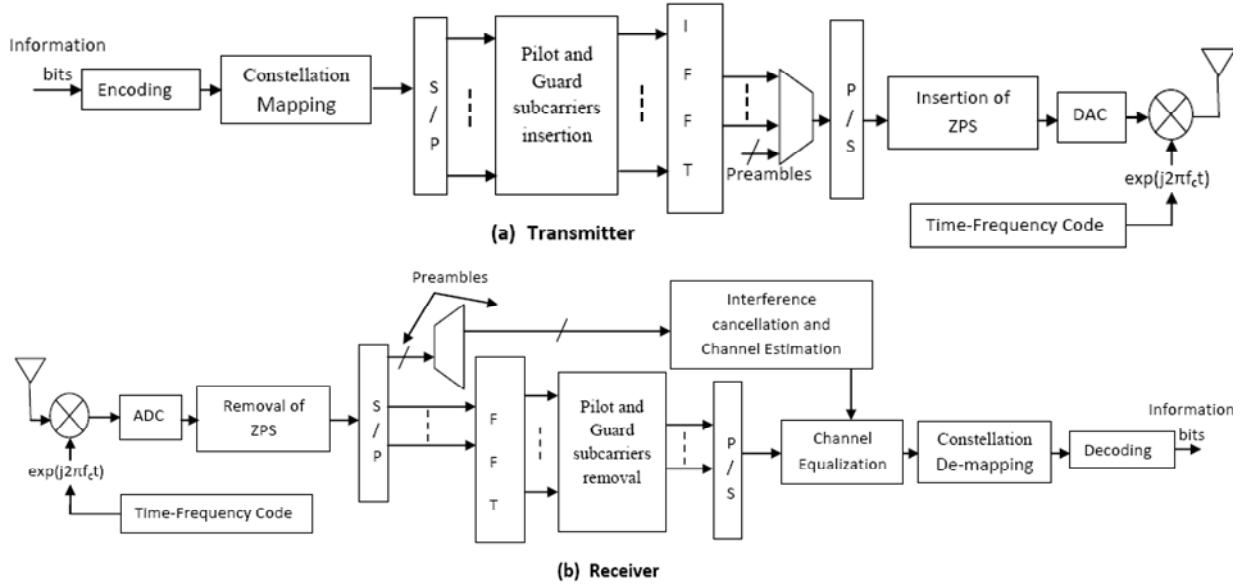


Figure 1. MB-OFDM system model.

interested in is IEEE 802.15.3a UWB RF channel model described in (Molisch et al., 2003) is given by,

$$h(t) = X \sum_{l=0}^{L_h} \sum_{k=0}^K \alpha_{k,l} \delta(t - T_l - \tau_{k,l}), \quad (4)$$

where  $T_l$ ,  $\tau_{k,l}$  and  $X$  are random variables representing the delay of the  $l$ -th cluster, the delay (relative to the  $l$ -th cluster arrival time) of the  $k$ -th multipath component of the  $l$ -th cluster and the log-normal shadowing, respectively. The channel coefficients are defined as a product of small-scale and large-scale fading coefficients, i.e.,  $\alpha_{k,l} = p_{k,l} \xi_l \beta_{k,l}$  where  $p_{k,l}$  takes on equiprobable  $\pm 1$  to account for signal inversion due to reflections, and  $\{\xi_l \beta_{k,l}\}$  are log-normal distributed path gains. Then we have  $E[\alpha_{k,l}(T_l, \tau_{k,l})] = 0$  and  $E[|\alpha_{k,l}(T_l, \tau_{k,l})|^2] = \Omega_0 e^{-T_l/\Gamma} e^{-\tau_{k,l}/\gamma}$ .  $\Gamma$  and  $\gamma$  are the cluster decay factor and ray decay factor, respectively. With different parameters, four typical environments are defined; they are CM1, CM2, CM3 and CM4. Details of the channel model are referred to in Molisch et al. (2003). Assuming perfect timing and frequency synchronization, the received time-domain signal (with ZPS) is given by,

$$\bar{y}_{ZPS} = \bar{d}_{ZPS} * \bar{h} + \bar{i}_{ZPS} + \bar{w}_{ZPS}, \quad (5)$$

where  $*$  denotes the convolution operator and  $\bar{h}$  is the channel response vector.  $\bar{w}_{ZPS}$  is the  $(N + Z) \times 1$  vector of Gaussian noise samples with zero-mean and variance equal to  $\sigma_w^2$ , and  $\bar{i}_{ZPS}$  is the  $(N + Z) \times 1$  vector of interference samples. In our model,  $\bar{i}_{ZPS}$  comprises the MAI and the NBI and so we write this vector as  $\bar{i}_{ZPS} = \bar{i}_{MA}^{ZPS} + \bar{i}_{NBI}^{ZPS}$ . The components of  $\bar{i}_{ZPS}$  are given by Batra et al. (2005),

$$i_{ZPS,m} = \sqrt{E_i} e^{j(2\pi f_i n T + \theta)}, \quad (6)$$

where  $E_i$  is the interference power,  $T$  is the original symbol period,  $\theta$  is a random phase that is distributed uniformly,  $u[-\pi, \pi]$ . The frequency of the interference is given by  $f_i$ , and is defined as

$$f_i = (m + \alpha) \frac{f_s}{N}, \quad 0 \leq m \leq N-2, \quad -0.5 \leq \alpha \leq 0.5, \quad (7)$$

where  $f_s$  is the sampling frequency,  $m$  is the subcarrier closest to the interference and  $\alpha$  is the position of interference between tones  $m - \frac{1}{2}$  and  $m + \frac{1}{2}$ . Inserting Equation (7) into (6) and using the fact that  $f_s = \frac{1}{T}$ , gives

$$i_{ZPS,m} = \sqrt{E_i} e^{j \frac{2\pi}{N} (m + \alpha) n + \theta}, \quad (8)$$

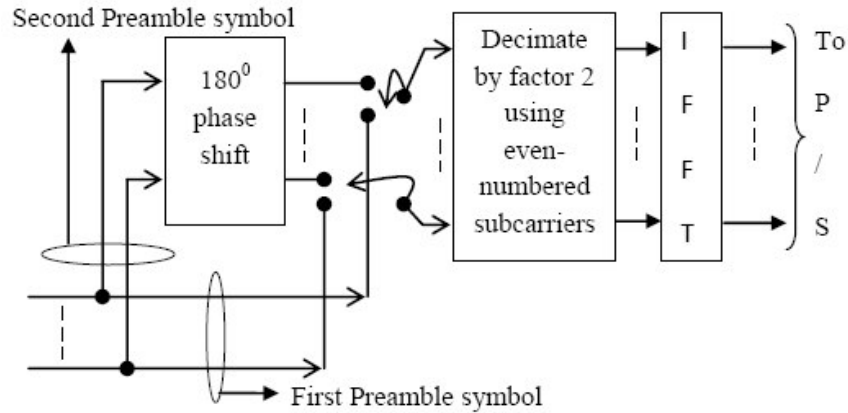


Figure 2. Construction of preambles, and stage of decimation.

The ZPS is removed from the received signal through overlapped-and-add (OLA) process, giving

$$\bar{y} = \bar{d} * \bar{h} + \bar{i} + \bar{w}, \tag{9}$$

where  $\bar{i}$  is the  $N \times 1$  vector of interference samples and  $\bar{w}$  is the  $N \times 1$  vector of noise samples with the same distribution as  $\bar{w}_{ZPS}$ . Two components of  $\bar{i}$  are  $\bar{i}_{MA}$  and  $\bar{i}_{NBI}$  and thus  $\bar{i} = \bar{i}_{MA} + \bar{i}_{NBI}$ . This signal is then converted into the frequency-domain with the FFT, to give

$$\bar{Y} = \mathbf{D}\bar{H} + \bar{I} + \bar{W}, \tag{10}$$

where  $\mathbf{D}$  is the  $N \times N$  diagonal matrix with the elements of  $\bar{\mathbf{D}}$  as diagonal elements that is,  $\mathbf{D} = \text{diag}(D_0, D_1, \dots, D_{N-1})$ . The symbols  $\bar{H}$ ,  $\bar{I}$  and  $\bar{W}$  are the frequency-domain representations of  $\bar{h}$ ,  $\bar{i}$ , and  $\bar{w}$  respectively. We also denote  $\bar{d} * \bar{h}$  as  $\bar{s}$  and  $\mathbf{D}\bar{H}$  as  $\bar{S}$ . Two components of  $\bar{I}$  are  $\bar{I}_{MA}$  and  $\bar{I}_{NBI}$  and thus  $\bar{I} = \bar{I}_{MA} + \bar{I}_{NBI}$ .

While data symbol is passed through the channel equalization block, it requires CIR from channel estimation block. For our system model, CIR is estimated using preamble symbols. Preambles must be free from MAI and NBI, since MAI and NBI affected preambles (in a similar manner in which data symbols are affected) will provide bad estimate of CIR. This will in turn result severe performance degradation in channel equalization and in data decoding. After synchronization sequence, preamble symbol of channel estimation sequence is sent to the receiver. So, the corresponding equations will be modified, during channel estimation, by plugging the

preamble symbol instead of data symbol. Suppose, frequency-domain preamble symbol is denoted by  $\bar{X}$  and given by,

$$\bar{X} = [X[k]]^T = [X_0, X_1, \dots, X_{N-1}]^T, \tag{11}$$

and the time-domain representation of  $\bar{X}$  is denoted by  $\bar{x}$ . Then Equation 9, for the received time-domain preamble symbol, can be written as

$$\bar{y} = \bar{x} * \bar{h} + \bar{i} + \bar{w} = \bar{r} + \bar{i} + \bar{w}, \tag{12}$$

where  $\bar{x} * \bar{h}$  is denoted as  $\bar{r}$ . Similarly, Equation 10 will be modified, to give frequency-domain received preamble symbol, as

$$\bar{Y} = \mathbf{X}\bar{H} + \bar{I} + \bar{W} = \bar{R} + \bar{I} + \bar{W} \tag{13}$$

where  $\mathbf{X}\bar{H}$  is denoted as  $\bar{R}$ . Note that the frequency-domain preamble sequence that is,  $\{X_0, X_1, \dots, X_{N-1}\}$  is defined in ECMA-368 standard. We need an IFFT operation, where necessary, to convert  $\bar{X}$  to  $\bar{x}$ , since ECMA-368 standardizes preamble sequences in frequency-domain. Conversely, FFT operation is applied on  $\bar{x}$  to revert back to  $\bar{X}$ .

### ANALYSIS OF PROPOSED TECHNIQUE

Tsai et al. (2008) used time-domain property of preamble sequence to get improved channel estimation. They used two preamble symbols of same sequences. However, the technique works to reduce only MAI. In this article, we use two preamble symbols of opposite, both in amplitude and phase, sequences. During the transmission of the second preamble, we must use a phase shifter to get the opposite sequence to that of first one, as shown in Figure 2. Our proposed technique comprises four steps. First,  $\bar{I}_{MA}$  is

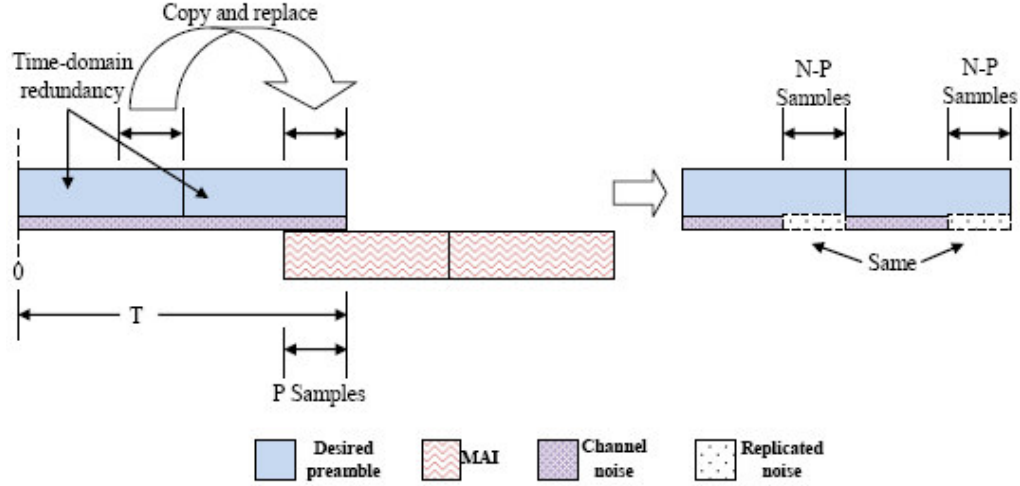


Figure 3. Adaptive select and replace (ASR) scheme.

reduced from both the preamble symbols through ASR scheme. Second,  $\bar{I}_{NBI}$  is cancelled through ASC scheme. Third, channels at odd-numbered subcarriers are found out by linear interpolation of least-squared (LS) estimated channels at even-numbered subcarriers. Lastly, estimation accuracy is enhanced further through frequency-domain filtering of estimated channel. However, the first thing to understand is the TR property. Basically, this is one of the properties of DFT (Proakis et al., 1995). The row vector representation of time-domain preamble sequence, denoted by  $x[n]$ , can be obtained by the IFFT operation on Equation 11 as

$$x[n] = \frac{1}{N} \sum_{k=0}^{N-1} X[k] \times e^{j2\pi kn/N}, \quad n = 0, 1, \dots, N-1 \quad (14)$$

By decimating the subcarriers in  $X[k]$  by a factor of 2, we get the corresponding time-domain preamble symbol as

$$x_{\text{even}}[n] = \frac{1}{2M} \sum_{k'=0}^{M-1} X[2k'] \times e^{j2\pi(2k')n/2M}, \quad n = 0, 1, \dots, N-1, \quad (15)$$

where  $M = N/2$ . The subscript “even” is used, since even-numbered subcarriers have been used during decimation. The odd-numbered subcarriers are set to zero. It must be noted that the last half of  $x_{\text{even}}[n]$  is the duplication of first half, since

$$\begin{aligned} x_{\text{even}}[n+M] &= \frac{1}{2M} \sum_{k'=0}^{M-1} X[2k'] \times e^{\frac{j2\pi(2k')(n+M)}{2M}} \\ &= \frac{1}{2M} \sum_{k'=0}^{M-1} X[2k'] \times e^{\frac{j2\pi(2k')n}{2M}} \times e^{j2\pi k'} \\ &= x_{\text{even}}[n], \quad n = 0, 1, \dots, M-1, \end{aligned} \quad (16)$$

Therefore, we have the TR property for the channel estimation preamble symbol. Similarly, the odd-numbered of subcarriers can

also be used to get TR property. However, we use even-numbered subcarriers in our study.

In the transmission side, we decimate two preamble symbols by a factor of 2 as shown in Figure 2. We must make the signal power, on each even-numbered subcarrier, doubled to maintain the same symbol energy. Using Equation 12, the first received time-domain preamble symbol can be given by,

$$\begin{aligned} \bar{y}_1 &= \bar{x}_1 * \bar{h} + \bar{i} + \bar{w}_1 \\ &= x_1 * \bar{h} + \bar{I}_{MA} + \bar{I}_{NBI} + \bar{w}_1, \end{aligned} \quad (17)$$

where subscript “1” has been used to indicate the first preamble symbol. The first term in Equation 17,  $\bar{x}_1 * \bar{h}$ , has also TR property, since  $\bar{x}_1$  has TR property and UWB channel model given first term in Equation 4 is time-invariant during the whole frame/packet transmission time. In addition,  $\bar{I}_{MA}$  exists in Equation 17, when the desired preamble symbol is collided with an interfering symbol. The power of  $\bar{I}_{MA}$  can be reduced by selecting the un-interfered part to replace the interfered samples. This MAI elimination process is adapted to the arrival time of interfering symbol, as shown in Figure 3. Assuming the timing information of MAI is available, the desired receiver can take the un-interfered time-domain samples to replace the redundant samples which have been interfered. If overlapping interval between the desired preamble and unexpected preamble is smaller than half of the symbol duration,  $T$ , the MAI can be completely eliminated. Conversely, If overlapping interval is equal or comparable to the symbol duration,  $T$ , there is no way to restore the desired preamble and . How much MAI,  $\bar{I}_{MA}$ , power will be tolerated is a system design issue. However, this adaptive select and replace (ASR) scheme will substantially reduce the power of the power of  $\bar{I}_{MA}$ . Thus, the application of ASR scheme on received preamble in Equation (17) results

$$\bar{y}_1 = \bar{x}_1 * \bar{h} + \bar{I}_{NBI} + \bar{w}_1, \quad (18)$$

A side effect is that ASR causes the repletion of part of the channel noise. This will increase the noise power. Conversely, the noise effect will be minimized, since only essential part which is contaminated by the interference is replaced. Note that we are copying the time-domain samples of NBI also. Yet this will not be a problem, since NBI will be cancelled from all of the subcarriers at the following stage of channel estimation. Similarly, we apply ASR scheme on the second received preamble symbol and obtain,

$$\bar{Y}_2 = \bar{X}_2 * \bar{H} + \bar{I}_{NBI} + \bar{W}_2, \tag{19}$$

where the subscript "2" has been used to indicate the second preamble symbol. Note the NBIs in both received preambles are the same, since we assume NBI is not intentional and thus it is stationary both in time- and frequency-domain.

We apply FFT operation on Equations 18 and 19 and convert time-domain received preamble symbols  $\bar{Y}_1$  and  $\bar{Y}_2$  into their corresponding frequency-domain symbols  $\bar{P}_1$  and  $\bar{P}_2$ , respectively. Thus,

$$\bar{P}_1 = \bar{X}_1 H + I_{NBI} + \bar{W}_1, \tag{20}$$

and,

$$\bar{P}_2 = \bar{X}_2 H + I_{NBI} + \bar{W}_2. \tag{21}$$

In Equation 21,  $\bar{X}_2 = -\bar{X}_1$ , since the preamble sequences are opposite both in amplitude and phase. Thus, we re-write Equation 21 as,

$$\bar{P}_2 = -\bar{X}_1 H + I_{NBI} + \bar{W}_2, \tag{22}$$

Adding Equations (20) and (22) and dividing the result by 2 gives,

$$\begin{aligned} \bar{A} &= \frac{\bar{P}_1 + \bar{P}_2}{2} = \frac{(\bar{X}_1 H + I_{NBI} + \bar{W}_1 - \bar{X}_1 H + I_{NBI} + \bar{W}_2)}{2} \\ &= I_{NBI} + \frac{(\bar{W}_1 + \bar{W}_2)}{2}, \end{aligned} \tag{23}$$

Subtracting Equation (22) from (20) and dividing the result by 2 gives,

$$\begin{aligned} \bar{B} &= \frac{\bar{P}_1 - \bar{P}_2}{2} = \frac{(\bar{X}_1 H + I_{NBI} + \bar{W}_1 - \bar{X}_1 H + I_{NBI} - \bar{W}_2)}{2} \\ &= \bar{X}_1 H + \frac{(\bar{W}_1 - \bar{W}_2)}{2} = \bar{H}_1 + \frac{(\bar{W}_1 - \bar{W}_2)}{2}, \end{aligned} \tag{24}$$

where the symbol  $\bar{H}$  has the same meaning as in Equation 13. In Equation 24,  $\bar{B}$  is nothing but the first received preamble symbol without interferences. Accordingly, we can use this preamble to estimate the channel.

Conversely,  $\bar{A}$  in Equation 23 is just the NBI with noise. Yet we do not know which subcarriers are affected by NBI. In fact, this knowledge can be used for weighting the received data symbol during soft-decision decoding. In addition to Equation 23 and 24, we need comparison step to detect the subcarriers affected by NBI. Thus, we are proposing addition, subtraction and comparison ASC scheme to cancel the NBI from preambles and to detect the affected subcarriers. The ASC scheme is depicted in Figure 4. In this figure, the symbol  $Y_{ik}$  represents the frequency-domain sample at a subcarrier  $k$  of  $i$ th received preamble symbol. The symbol

$B_k$  indicates  $\bar{B}$  at subcarrier  $k$ . Let us consider this particular subcarrier  $k$ , at which there is no NBI component. This causes  $Y_{1k}$  and  $B_k$  to contain only the signal and noise. Consequently, they have the same power (in a comparable sense). We can determine a low threshold  $\gamma$  that is based on desired signal power, noise variance and pre-knowledge of channel environment. Thereafter, we set the following condition onto the subcarrier,

$$|Y_{1k} - B_k| > \gamma, \tag{25}$$

If this inequality is satisfied, then the power of  $A_k$  ( $\bar{A}$  at subcarrier  $k$ ) is measured to get an estimate of the NBI-component at subcarrier  $k$ . This process is repeated for each even-numbered subcarrier.

We know that  $\bar{B}$  in Equation 24 is the first received preamble symbol without interferences. Conversely,  $X_1$  is the diagonal matrix whose diagonal elements constitute the first transmitted preamble symbol. The second term,  $\frac{(\bar{W}_1 - \bar{W}_2)}{2}$ , is nothing but the additive white Gaussian noise (AWGN). By using least-square (LS) criteria, we have the LS estimation for  $\bar{H}$  (Kay, 1993),

$$\hat{H}_{LS} = (X_1^H \times X_1)^{-1} X_1^H \bar{B}, \tag{26}$$

where  $X_1^H$  is the Hermitian matrix of  $X_1$ . Since  $X_1$  is a diagonal matrix, we have the estimated channel gain of subcarrier  $k$  being,

$$\hat{H}_{LS}[k] = \frac{B_k}{X_k}, \tag{27}$$

where  $X_k$  is the transmitted preamble at subcarrier  $k$ . Note that other estimation approaches such as LMMSE, and low rank LMMSE can also be used; we use LS approach because of its low computational complexity.

Using Equation 27, we get the LS estimated channels at every even-numbered subcarrier. We still do not obtain the channel information at odd-numbered subcarriers, since we performed frequency-domain decimation and inserted zeros there. So, we apply linear interpolation to get the channel gains in odd-numbered subcarriers. Thus, we have the channel gains

$$\hat{H} = \begin{cases} \hat{H}_{LS}[k] = \frac{B_k}{X_k}, & k \in \text{even} \\ \hat{H}_{IP}[k] = \frac{\hat{H}_{LS}[k-1] + \hat{H}_{LS}[k+1]}{2}, & k \in \text{odd and } k \neq N-1; \\ \hat{H}_{IP}[k] = \hat{H}_{LS}[N-2], & k = N-1 \end{cases} \tag{28}$$

where the subscript "IP" is used to indicate interpolation. Instead of linear interpolation higher order polynomial interpolation can also be used. Let us call the channel estimation using Equation 28 "LS-ASR-ASC scheme". If we do not use ASR and ASC schemes, channel interpolation is not required; channel information at all subcarriers is available. In this article, LS estimation without interpolation (that is, without ASR and ASC schemes) is termed conventional LS, or simply LS, estimation.

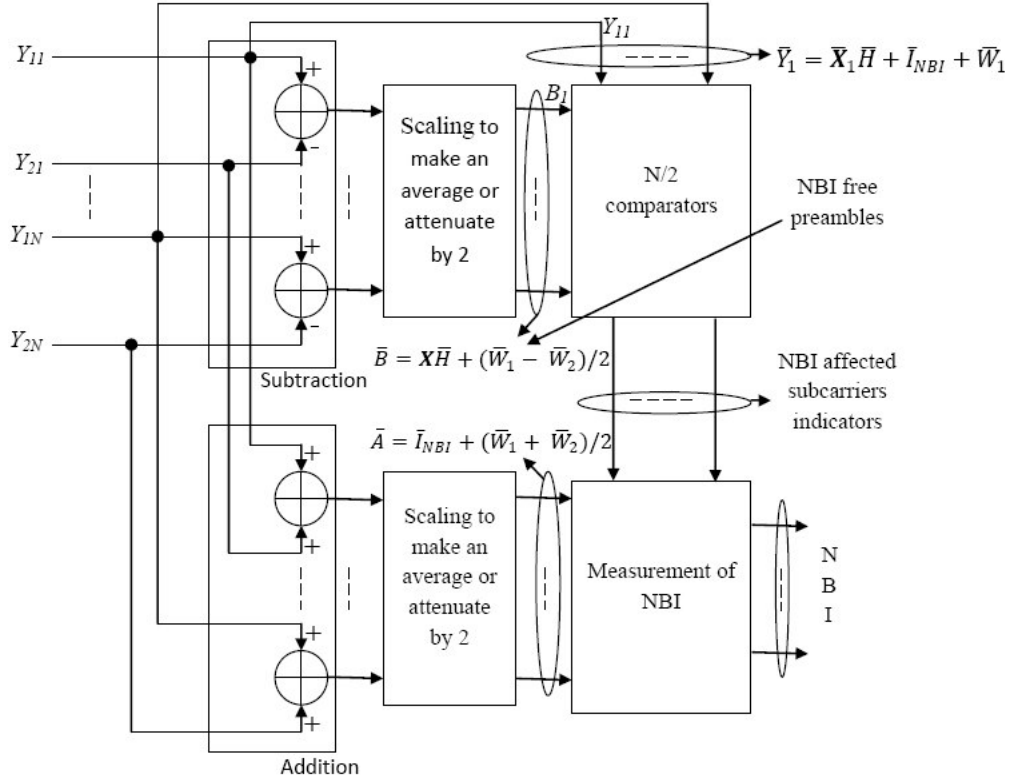


**Figure 4.** Addition, subtraction and compare (ASC) scheme.

In this stage, we improve the estimated channel, obtained in Equation 28, using the power delay profile of the received channel. The correlation of the transmitted preamble sequence with the received preamble sequence provides an estimate of the PDP. Accordingly, we estimate the PDP for each band by

$$P_z = \sum_{i=1}^2 \left| \sum_{j=z}^{z+N} y_{i,j} \times x_{i,j-z} \right|^2, \quad (29)$$

where  $P_z$  is the power of the  $z$ th delay path,  $z = 0, 1, \dots, Z$  and  $x_{i,j}$  is the  $j$ th sample of the  $i$ th transmitted time-domain preamble symbol;  $y_{i,j}$  is the  $j$ th sample of the  $i$ th received time-domain preamble symbol. Now, we generate the profile vector given by,

$$g_z = \begin{cases} 1, & P_z \geq \frac{1}{K} \max\{P_z\}_0^{Z-1} \\ 0, & P_z < \frac{1}{K} \max\{P_z\}_0^{Z-1} \end{cases} \quad (30)$$

where  $\max\{P_z\}_0^{Z-1}$  stands for the maximum value of  $P_z$  over  $z = 0, 1, \dots, Z$  and  $K$  is a heuristic threshold factor. We pad zeros and apply  $N$ -point FFT on the resultant vector to get the

frequency-domain filter coefficients. Next, we use these coefficients to filter the channel gains obtained in Equation 28. Let us denote the vector, containing the frequency-domain filter coefficients, by  $G_z$ . Thus, our proposed technique finally provides the estimated channels by,

$$\tilde{H}_{Filtered} = G_z \otimes \tilde{H}, \quad (31)$$

where the operator  $\otimes$  represents the circular convolution. Let us call the channel estimation using Equation 31 “LS-ASR-ASC-CF scheme”.

Now, we analyze the computational complexity issue of the technique through intuitional approach. The number of multiplication is considered as the source of computational complexity. The conventional LS estimation requires  $N$  multiplication, where  $N$  is the FFT size. Let us find out the complexity of our proposed technique in two steps. First, The LS-ASR-ASC scheme needs only  $N/2$  multiplications, since estimation is performed at only even-numbered subcarriers and ASR/ASC does not use any multiplication. Second, no supplementary hardware complexity is required for PDP estimation, since the correlator structure is already used for synchronization. Therefore, the bulk of the additional complexity comes from the implementation of the frequency-domain filters. An  $N$ -tap complex filter requires  $4N$  multipliers. If the filter has symmetric complex coefficients, the required number of multipliers is reduced to  $2N$ .

**Table 1.** UWB Channel characteristics and corresponding model parameters.

Target channel characteristics and Model parameters	CM1	CM2
	Line of sight (LOS): -4m	Non-line of sight (NLOS): -4m
Mean excess delay (ns)	5.0	9.94
RMS delay (ns)	5.0	8
Cluster arrival rate (1/ns)	0.0233	0.4
Ray arrival rate (1/ns)	2.5	0.5
Cluster decay factor	7.1	5.5
Ray decay factor	4.3	6.7
Standard deviation (SD) of cluster lognormal fading term (LNFT) (dB)	3.3941	3.3941
SD of ray LNFT (dB)	3.3941	3.3941
SD of LNFT for total multi-path realization (dB)	3	3

**Table 2.** Channel estimation preamble related simulation parameters.

Parameter	Specification
Frequency bands	Group 1 (band #1-3)
Sampling frequency	528 MHz
FFT size	128
IFFT and FFT period	242.42 (ns)
Number of samples in ZPS	37
ZPS duration in time	70.08 (ns)
Symbol interval	312.5 (ns)
Duration of the channel estimation sequence	6 × 312.5 (ns) = 1.875 (µs)

Thus, the LS-ASR-ASC-CF scheme requires  $2 \times N + \frac{N}{2} = \frac{5 \times N}{2}$  multiplications. We observe that the complexity of our proposed technique is just 2.5 times that of LS estimation. Note that the computational complexity of LMMSE is  $N^3 + 2 \times N^2$  (Noh et al., 2006) which is much higher.

### SIMULATION RESULTS

Computer simulation is performed to evaluate the system performances. We use MATLAB as simulation software. The target UWB channel models are CM1 and CM2. Parameters associated with these models are listed in Table 1. We quantize time in the continuous-time model's (time, value) pairs and hence discrete time model is realized, since the output of the model is a continue time arrival and amplitude value. Frequency hopped (FH) point to point communication is simulated using three frequency bands, where the first symbol is transmitted on a centre frequency of 3432 MHz, the second symbol is

transmitted on a centre frequency of 3960 MHz, the third symbol is transmitted on a centre frequency of 4488 MHz, the forth symbol is transmitted on a center frequency of 3432 MHz, and so on. All other preamble (for channel estimation) related parameters are selected according to specifications (ECMA International, 2008) and are shown in Table 2. Simulation results are found from the average of 1000 realizations. Note that we use 15-tap symmetric complex filter in LS-ASR-CF scheme in our simulation, since it is the optimum number of taps without any detectable system performance loss (Png et al., 2008). We consider the conventional LS estimation as a reference estimator for the performance comparison. Figures 5 to 7 presents the normalized mean square error (NMSE) performances of our proposed techniques working under different interfering environments. Note that we define NMSE as,

$$NMSE = \frac{\sum_{k=0}^{N-1} |Estimated\ channel\ at\ subcarrier\ k - True\ Channel\ at\ subcarrier\ k|^2}{\sum_{k=0}^{N-1} |True\ Channel\ at\ subcarrier\ k|^2}, \quad (32)$$

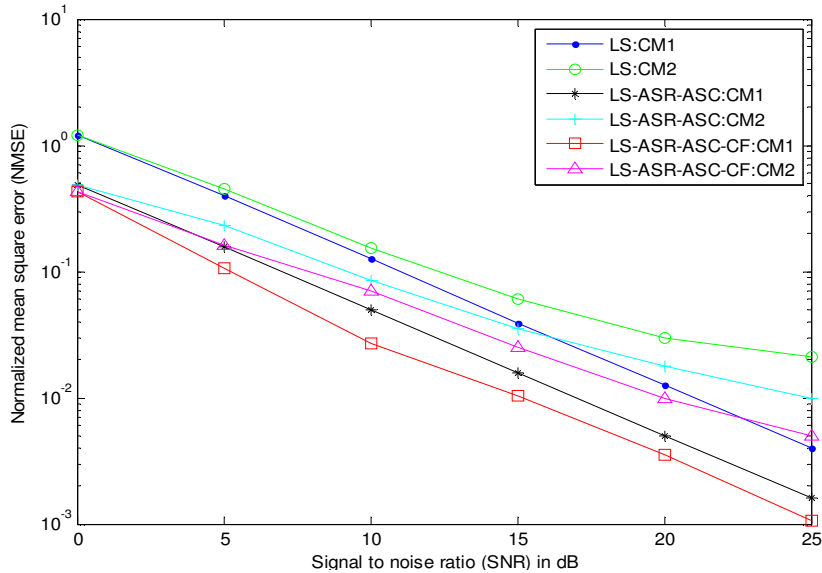


Figure 5. NMSE versus SNR for an interference-free channel.

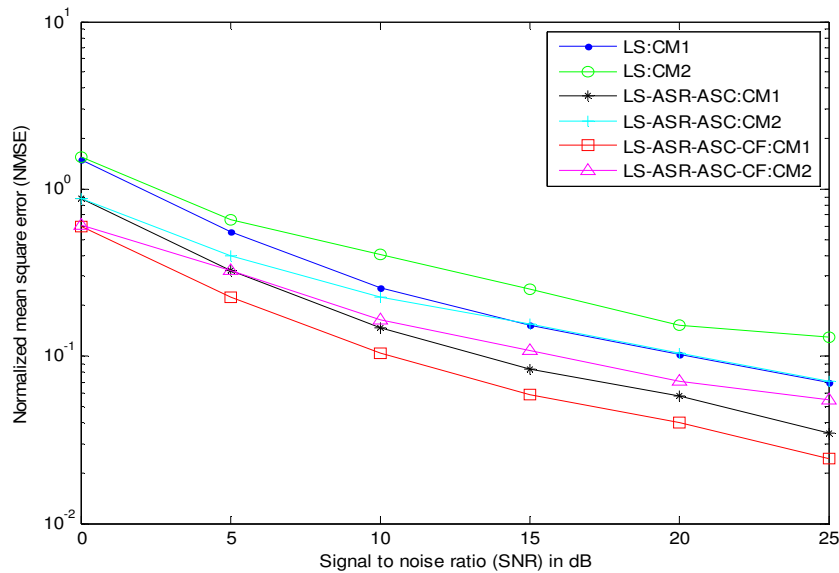


Figure 6. NMSE versus SNR for SIR= 10 dB.

Figure 5 shows the NMSE versus signal-to-noise ratio (SNR) for an interference-free channel. It shows that our proposed channel estimation schemes outperform the conventional LS estimation method, since power on each even-numbered subcarrier is doubled. We observe that LS-ASR-ASC scheme outperform the reference estimator by almost 4 dB SNR advantage in CM1 environment. However, the SNR advantage in CM2 is 3 dB. Caused by somewhat larger interpolation error, the SNR advantage in CM2 is reduced. Interpolation error in CM1 is relatively

smaller than that in CM2, since the correlation between neighboring subcarriers in CM2 is comparatively lower than that in CM1. We also observe that LS-ASR-ASC-CF scheme gives further SNR improvement in both CM1 and CM2, since filter coefficients is directly derived from channel's power delay profile.

In Figure 6, we show the NMSE versus SNR for signal-to-interference ratio (SIR) of 10 dB that is, a moderate interfering environment. We observe that the NMSE is increased in every case, with performance saturation at

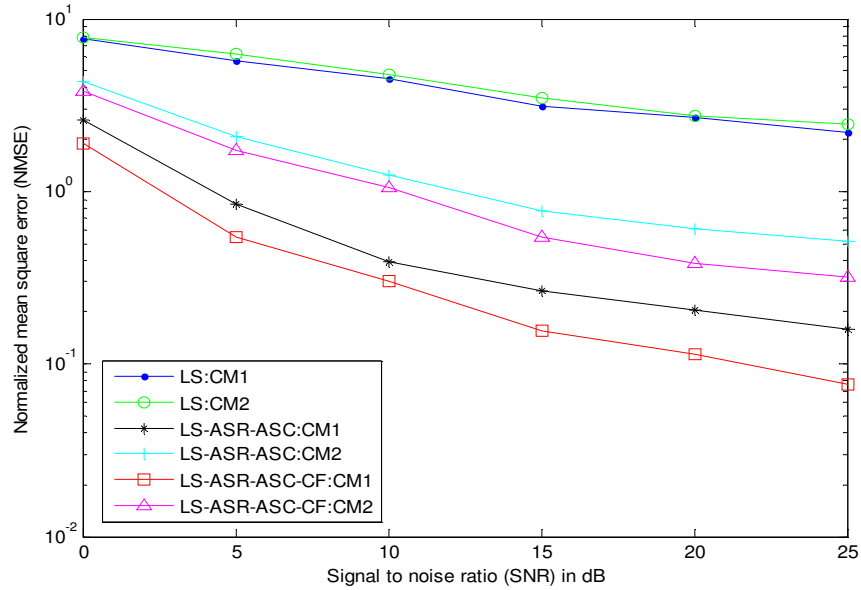


Figure 7. NMSE versus SNR for SIR= -3 dB.

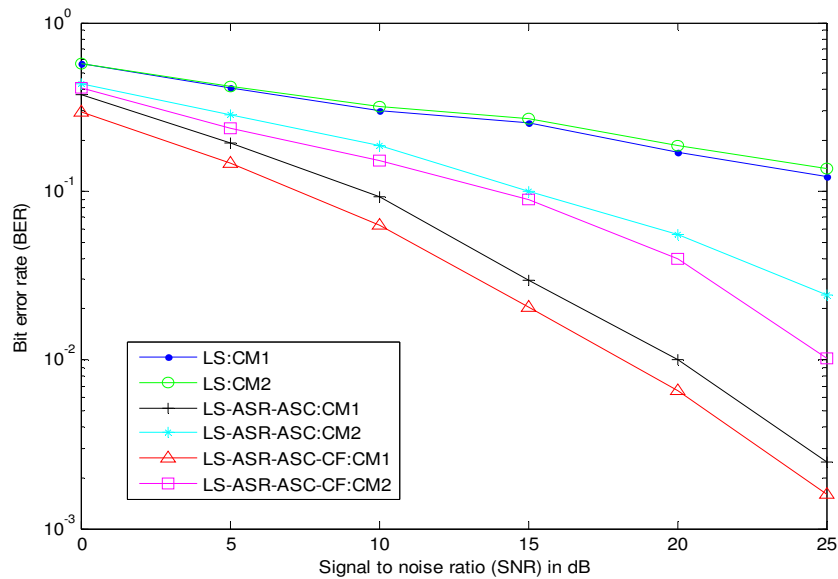


Figure 8. Unencoded BER performances for SIR= -3 dB.

very high SNR. The SNR improvements by our proposed schemes are comparatively less at low SNR than that at high SNR, since ASR scheme can eliminate the multi-access interference at the cost of AWGN enhancement.

Figure 7 shows the NMSE versus SNR for SIR= -3 dB that is, severe interfering environment. This figure noticeably evidences the effectiveness of our proposed channel estimation approach. We see that the performance of conventional LS estimation approach is

severely degraded by the interference. However, the performances of LS-ASR-ASC and LS-ASR-ASC-CF schemes are still far better for both CM1 and CM2.

In addition to NMSE performances, we also compare the unencoded bit error rate (BER) performances of the system employing our channel estimation schemes. This is presented in Figure 8. The system employing conventional LS estimation approach is utterly a failure in providing an acceptable BER performance, since the

channel is equalized by an improper estimated channel. On the other hand, the system employing LS-ASR-ASC or LS-ASR-ASC-CF scheme provides a satisfactory BER performance, since the channel estimation is done using interference-free (interference power is substantially reduced) preambles. Note that we use QPSK modulation for constellation mapping. The number of data subcarriers, pilot subcarriers and guard subcarriers are 100, 12 and 10, respectively.

## Conclusion

In this article, we propose a preamble-based energy-efficient channel estimation method for MB-OFDM UWB system in presence of MAI and NBI. This technique cancels MAI and NBI from preambles by introducing TR property into preamble symbols and by using the opposite sequences in preambles, respectively. PDP-driven frequency-domain filtering of LS estimated channels, using interference-free preambles, provides a further improvement in the estimation accuracy. This synergy-based technique offers satisfactory NMSE and BER performances in a severe interfering environment, whereas the conventional LS estimation gives extremely bad performances. Even in an interference-free channel, our proposed technique outperforms the LS estimation approach. This method is highly energy-efficient, since it provides sufficient SNR-advantage in both CM1 and CM2 environments. Moreover, when we compare our technique to LS approach, the computational complexity is not much higher. Therefore, the proposed channel estimation technique can effectively be used in MB-OFDM UWB system.

As a future work, the estimation accuracy of our technique would be investigated for imperfect symbol timing and carrier frequency synchronization. The work towards a modification of this channel estimation technique for an impulsive noisy environment (Middleton, 1999) would also be a part of future extensions of our work.

## ACKNOWLEDGEMENT

This research was supported by the Ministry of Knowledge Economy (MKE), Korea, under the Information Technology Research Centre (ITRC) support program supervised by the National IT Industry Promotion Agency (NIPA) (NIPA-2010-C1090-1011-0007).

## REFERENCES

- Batra A, Zeidler JR (2005). Narrowband Interference Mitigation in OFDM Systems. In Proceedings of IEEE MILCOM, San Diego, USA, pp. 1-7.
- ECMA International (2008). Standard ECMA-368: High Rate Ultra Wideband PHY and MAC Standard, ECMA International, 2<sup>nd</sup> Edition.
- Fan X, Leng B, Zhang Z, Bi G (2005). An Improved Channel Estimation Algorithm for OFDM UWB. WCNC, New Orleans, LA, USA, Proc. IEEE, 1: 173-176.
- Hadaschik N, Zakia I, Ascheid G, Meyr H (2007). Joint Narrowband Interference Detection and Channel Estimation for wideband OFDM, In Proceedings of the European Wireless Conference.
- Kay SM (1993). Fundamentals of Statistical Signal Processing: Estimation Theory, Prentice Hall International, Inc., New Jersey, USA, pp. 219-275.
- Li Y, Minn H, Rajatheva RMAP (2008). Synchronization, Channel Estimation and Equalization in MB-OFDM Systems. IEEE Trans. Wireless Commun., 7(11): 4341-4352.
- Li Y, Molisch AF, Zhang J (2006). Practical Approaches to Channel Estimation and Interference Suppression for OFDM-based UWB Communications. IEEE Trans. Wireless Commun., 5(9): 2317-2320.
- Middleton D (1999). Non-Gaussian Noise Models in Signal Processing for Telecommunications: New Methods and Results for Class A and Class B Noise Models, IEEE Trans. Inf. Theory, 45(4): 1129-1149.
- Molisch A, Foerster J, Pendergrass M (2003). Channel Models for Ultra-wideband Personal Area Networks, IEEE Commun. Mag., 10(6): 14-21.
- Noh M, Lee Y, Park H (2006). Low Complexity LMMSE Channel Estimation for OFDM, IEEE Proc. Commun., 153(5): 645-650.
- Png KB, Peng X, Chin F. (2008). A Low Complexity Adaptive Channel Estimation Scheme for MB-OFDM System. Proc. IEEE ICUWB, Germany, 3: 47-50.
- Proakis JG, Manolakis DG (1995). Digital Signal Processing: Principles, Algorithms and Applications, Prentice Hall, 3rd Edition, pp. 394-425.
- Shin S, Yang Q, Kwak KS (2007). Performance Analysis of MB-OFDM System using SVD Aided LMMSE Channel Estimation. Proc. IEEE ICUWB, Singapore, pp. 840-844.
- Tsai YR, Wang CC, Li XS (2008). Adaptive Channel Estimation for MB-OFDM Systems in Multi-access Interfering Environments. Proc. IEEE VTC, Singapore, pp. 918-922.